PHYSICAL REVIEW B **80**, 020505(R) (2009)

f-spin physics of rare-earth iron pnictides: Influence of *d*-electron antiferromagnetic order on the heavy-fermion phase diagram

Jianhui Dai,[1] Jian-Xin Zhu,[2] and Qimiao Si[3]
[1]*Zhejiang Institute of Modern Physics, Zhejiang University, Hangzhou 310027, China*
[2]*Theoretical Division, Los Alamos National Laboratory, Los Alamos, New Mexico 87545, USA*
[3]*Department of Physics and Astronomy, Rice University, Houston, Texas 77005, USA*
(Received 10 March 2009; revised manuscript received 5 June 2009; published 24 July 2009)

Some of the high-T_c iron pnictides contain magnetic rare-earth elements, raising the question of how the existence and tunability of a *d*-electron antiferromagnetic order influences the heavy-fermion behavior of the *f* moments. With CeOFeP and CeOFeAs in mind as prototypes, we derive an extended Anderson lattice model appropriate for these quaternary systems. We show that the Kondo screening of the *f* moments are efficiently suppressed by the *d*-electron ordering. We also argue that, inside the *d*-electron ordered state (as in CeOFeAs), the *f* moments provide a rare realization of a quantum frustrated magnet with competing J_1-J_2-J_3 interactions in an effective square lattice. Implications for the heavy-fermion physics in broader contexts are also discussed.

DOI: 10.1103/PhysRevB.80.020505 PACS number(s): 74.70.Tx, 75.10.−b, 71.10.Hf, 71.27.+a

The homologous rare-earth iron arsenides exhibit antiferromagnetic (AF) ground states in addition to the high-temperature superconductivity.[1–5] The systems of interest here are the arsenides $RO_xF_{1-x}FeAs$, with R=Ce, Sm, Nd, Pr,… being magnetic rare earths, which have superconducting transition temperatures higher[2–5] than the maximal $T_c \approx 26$ K of $LaO_xF_{1-x}FeAs$.[1] The parent compounds of these systems, *R*OFeAs, have a layered structure, with FeAs and *R*O layers sandwiching each other. They typically show a collinear AF order and a structure distortion, which are successively suppressed by carrier doping in favor of superconductivity.[6] Also of interest are the iron phosphides. LaOFeP was the iron pnictide reported to show superconductivity below $T_c \approx 4$ K.[7] This compound has the same layered structure as LaOFeAs but does not order magnetically.[8]

The distinction between the iron phosphides and arsenides becomes even more pronounced when La is replaced by Ce. CeOFeP is neither superconducting nor magnetically ordered, and its Ce *f* electrons exhibit heavy-fermion behavior with a Kondo temperature $T_K \approx 10$ K.[9] CeOFeAs has the *d*-electron collinear AF ordering below $T_N^{(d)} \approx 130$ K. Its *f* electrons display a noticeable AF order below $T_N^{(f)} \approx 4$ K (Refs. 2 and 10) but does not show any heavy-fermion features. What underlies the heavy-fermion behavior in CeOFeP and its absence in CeOFeAs? One possibility is that this primarily reflects the very different interlayer $3d$-$4f$ couplings between CeOFeP and CeOFeAs, as suggested by a first-principles LDA+DMFT study.[11] However, a more complete theoretical estimate using a full density of states, which is strongly peaked away from the Fermi energy, suggests that the effective Kondo couplings in CeOFeP and CeOFeAs may in fact be comparable.[12] Muon-spin-relaxation and neutron-scattering experiments[13,14] may also be interpreted in terms of a sizable Kondo coupling in CeOFeAs.

In this Rapid Communication, we discuss the possibility that the distinction in the *d*-electron magnetism between CeOFeP and CeOFeAs plays an important role in influencing their heavy-fermion behavior. This mechanism is expected to play an especially important role when we consider not only the end materials CeOFeP and CeOFeAs but also the series $CeOFeAs_{1-x}P_x$, which has been proposed to realize a continuously varying *d*-electron AF order and the associated quantum critical point.[15]

Studying the effect of the *d*-electron AF order on the heavy-fermion phase diagram not only sheds light on the properties of the iron pnictides but also represents a twist to the heavy-fermion physics in general. Typically, AF order in heavy-fermion metals is induced by the Ruderman-Kittel-Kasuya-Yosida (RKKY) interactions among the *f* moments, and the heavy-fermion phase diagram involves the competition between RKKY and Kondo coupling.[16,17] A tunable *d*-electron AF order adds a dimension to the heavy-fermion phase diagram.

In the following, we will consider this effect within an extended Anderson lattice model (ALM) appropriate for the stoichiometric *R*-1111 compounds *R*OFe*X* (*X*=As or P). The model incorporates the interlayer hybridization between pnictogen *X* *p* orbitals and rare-earth *R* *f* orbitals. We note in passing that the derived model takes into account the microscopic crystal structure and symmetry of the *R*-1111 compounds. Given that there are many materials of the same ZrCuSiAs-type structure,[18] with many of them containing magnetic rare-earth elements, we expect that our model will also be germane to many such related compounds.[19]

General considerations. The lattice structure of the *R*-1111 compound series is schematically shown in Fig. 1. Let Fe atoms be in the (x,y) plane with the coordinate $(\vec{r},0)$, where $\vec{r}=(i_x,i_y)$, where i_x and i_y are both integers (the nearest Fe-Fe distance is set to unity). The coordinates of *X* and *R* atoms are $(\vec{r}_p,\eta z_p)$ and $(\vec{r}_f,\eta z_f)$, respectively, where $\vec{r}_p=(i_x+1/2,i_y+1/2)$, $\vec{r}_f=(i_x-1/2,i_y+1/2)$, $\eta=e^{i\pi(i_x+i_y)}$, and z_p and z_f are the distances of *X* and *R* atoms to the Fe plane. We denote the *d*, *p*, and *f* electrons by $d_\sigma^{(\alpha)}(\vec{r})$, $p_\sigma^{(\mu)}(\vec{r}_p,\eta z_p)$, and $f_\sigma^{(m)}(\vec{r}_f,\eta z_f)$, with orbital indices $\alpha=d_{xy},d_{xz},d_{yz},d_{x^2-y^2},d_{3z^2-r^2}$, $\mu=p_x,p_y,p_z$, and $m=1,\ldots,l$.

The model Hamiltonian. The hybridization part of the Hamiltonian is given by $H_{hybrid}=H_{pd}+H_{pf}$, where

$$H_{pd}=\sum_{\vec{r}} V_{pd}^{(\mu,\alpha)}[p_\sigma^{(\mu)\dagger}(\vec{r}_p,\eta z_p)D_\sigma^{(\alpha)}(\vec{r})+\text{H.c.}], \qquad (1)$$

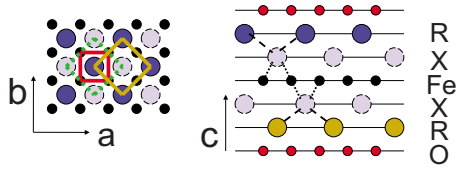

FIG. 1. (Color online) The lattice structure of *R*-1111 series. The small black and red (connected with solid line) circles represent Fe and O ions, respectively, and the big blue and brown and dashed gray circles are the *R* and *X* ions, respectively. The small solid red, large solid brown, and dotted green squares describe the Fe, *R*, and *X* plaquettes, respectively. Left panel: *ab* plane; right panel: *ac* plane. The dashed and dotted lines denote V_{pf} and V_{pd}, respectively.

$$H_{pf} = \sum_{\vec{r}} V_{pf}^{(\mu,m)} [p_\sigma^{(\mu)\dagger}(\vec{r}_p, \eta z_p) F_\sigma^{(m)}(\vec{r}_f, \eta z_f) + \text{H.c.}]. \quad (2)$$

Here we introduce

$$D_\sigma^{(\alpha)}(\vec{r}) = \sum_{\square} d_\sigma^{(\alpha)}(\vec{r}) \equiv d_\sigma^{(\alpha)}(i_x, i_y) + d_\sigma^{(\alpha)}(i_x+1, i_y) + d_\sigma^{(\alpha)}(i_x, i_y+1) + d_\sigma^{(\alpha)}(i_x+1, i_y+1)$$

and

$$F_\sigma^{(m)}(\vec{r}_f, \eta z_f) = \sum_{\square} f_\sigma^{(m)}(\vec{r}_f, \eta z_f) \equiv f_\sigma^{(m)}(i_x - 1/2, i_y + 1/2, \eta z_f) + f_\sigma^{(m)}(i_x + 3/2, i_y + 1/2, \eta z_f) + f_\sigma^{(m)}(i_x + 1/2, i_y - 1/2, \eta z_f) + f_\sigma^{(m)}(i_x + 1/2, i_y + 3/2, \eta z_f)$$

as the plaquette operators of d and f electrons around X atoms. (Summations over the repeated spin and channel indices are implied hereafter unless otherwise specified.)

The interaction part of the Hamiltonian, $H_{int} = H_{int,d} + H_{int,p} + H_{int,f}$, contains the usual on-site Coulomb interactions (U_p, U_d, and U_f) and the Hund's coupling ($J_{H,d}$). The total Hamiltonian is then $H = H_0 + H_{hybrid} + H_{int}$, with H_0 containing the primitive site energies of d, p, and f electrons denoted by $\varepsilon_d^{(\alpha)}$, $\varepsilon_p^{(\mu)}$, and $\varepsilon_f^{(m)}$, respectively.

It is expected that U_p is small compared to the other Coulomb interactions. We will therefore set $U_p = 0$ in which case the p orbitals can be readily integrated out. The obtained effective Hamiltonian $\tilde{H}$ takes the form

$$\tilde{H} = H_0 + H_d + H_f + H_{df} + H_{int,d} + H_{int,f}. \quad (3)$$

Here $H_d = \Sigma_{\vec{r}} V_d^{(\alpha\alpha')} [D_\sigma^{(\alpha)\dagger}(\vec{r}) D_\sigma^{(\alpha')}(\vec{r}) + \text{H.c.}]$, $H_f = \Sigma_{\vec{r}} V_f^{(mm')} [F_\sigma^{(m)\dagger}(\vec{r}_f, \eta z_f) F_\sigma^{(m')}(\vec{r}_f, \eta z_f) + \text{H.c.}]$, and $H_{df} = \Sigma_{\vec{r}} V_{df}^{(\alpha m)} [D_\sigma^{(\alpha)\dagger}(\vec{r}) F_\sigma^{(m)}(\vec{r}_f, \eta z_f) + \text{H.c.}]$, with $V_d^{(\alpha\alpha')} = -\Sigma_\mu V_{pd}^{(\mu,\alpha)} V_{pd}^{(\mu,\alpha')} / \varepsilon_p^{(\mu)}$, $V_f^{(mm')} = -\Sigma_\mu V_{pf}^{(\mu,m)} V_{pf}^{(\mu,m')} / \varepsilon_p^{(\mu)}$, $V_{df}^{(\alpha m)} = -\Sigma_\mu V_{pd}^{(\mu,\alpha)} V_{pf}^{(\mu,m)} / \varepsilon_p^{(\mu)}$. In the momentum $\mathbf{K}$ space (in the reduced Brillouin zone corresponding to two Fe atoms in the conventional cell with lattice constant $a = \sqrt{2}$), $H_d = \Sigma_{\mathbf{K}} V_d^{(\alpha\alpha')} g_d^{(\eta\eta')}(\mathbf{K}) d_{\eta\mathbf{K}\sigma}^{(\alpha)\dagger} d_{\eta'\mathbf{K}\sigma}^{(\alpha')}$, $H_f = \Sigma_{\mathbf{K}} V_f^{(mm')} g_f(\mathbf{K}) f_{\eta\mathbf{K}\sigma}^{(m)\dagger} f_{\eta\mathbf{K}\sigma}^{(m')}$, and $H_{df} = \Sigma_{\mathbf{K}} V_{df}^{(\alpha m)} g_{df}^{(\eta\eta')}(\mathbf{K}) [d_{\eta\mathbf{K}\sigma}^{(\alpha)\dagger} f_{\eta'\mathbf{K}\sigma}^{(m)} + \text{H.c.}]$, where $d_{\eta\mathbf{K}\sigma}^{(\alpha)}$ and $f_{\eta\mathbf{K}\sigma}^{(m)}$ are the Fourier transform of d- and f-electron operators in the sublattices $\eta = A$ or B, respectively. The $\mathbf{K}$ dependence of the dispersions and d-f hybridization is only encoded in the form factors, given by $g_d^{(AA)}(\mathbf{K}) = g_d^{(BB)}(\mathbf{K}) = 4 + 2\cos(K_x a)\cos(K_y a)$, $g_d^{(AB)}(\mathbf{K}) = g_d^{(BA)}(\mathbf{K}) = 8\cos(K_x a/2)\cos(K_y a/2)$, $g_f(\mathbf{K}) = 16\cos^2(K_x a/2)\cos^2(K_y a/2)$, $g_{df}^{(AA)}(\mathbf{K}) = g_{df}^{(BB)}(\mathbf{K}) = 8\cos^2(K_x a/2)\cos(K_y a/2)$, $g_{df}^{(BA)}(\mathbf{K}) = g_{df}^{(BA)}(\mathbf{K}) = 8\cos(K_x a/2)\cos^2(K_y a/2)$.

The d-electron correlations. For moderate large U_d, we may start from the strong-coupling limit yielding the frustrated J_1-J_2 Heisenberg model for the d electrons.[20–22] The itinerancy of the d electrons will further reduce the ordered moments and eventually lead to a paramagnetic phase.[15] In fact, both the weak- and strong-coupling limits suggest that the staggered magnetization $M_d = \Sigma_\alpha M_d^{(\alpha)} = -(1/N)\Sigma_{\mathbf{K}} \langle \{ d_{\eta\mathbf{K}\uparrow}^{(\alpha)\dagger} d_{\eta\mathbf{K}+\mathbf{Q}\uparrow}^{(\alpha)} - d_{\eta\mathbf{K}\downarrow}^{(\alpha)\dagger} d_{\eta\mathbf{K}+\mathbf{Q}\downarrow}^{(\alpha)} \} \rangle$ is a dominating order parameter, with $Q = (\pi, \pi)$ and N being the number of $\mathbf{K}$ points in the reduced Brillouin zone. For the purpose of demonstrating the effect of d-electron order on the Kondo effect, we treat $M_d^{(\alpha)}$ as the mean-field parameters and approximate $H_{int,d}$ by $J_d \Sigma_{\mathbf{K}} \sigma M_d^{(\alpha)} [d_{\eta\mathbf{K}\sigma}^{(\alpha)\dagger} d_{\eta\mathbf{K}+\mathbf{Q}\sigma}^{(\alpha)} + \text{H.c.}]$, with J_d being the effective coupling strength. The AF ordering gap, $\Delta_{AF}^{(\alpha)} = J_d M_d^{(\alpha)}$, is sizable for FeAs but vanishes for FeP.

Kondo effect vs d-electron ordering. In order to understand the competition between the Kondo effect and d-electron AF order, we first neglect the f-electron ordering. We are then led to consider

$$\begin{aligned} H_{ALM} = & \sum_{\mathbf{K}} [\varepsilon_d^{(\alpha)} \delta_{\alpha\alpha'} \delta_{\eta\eta'} + V_d^{(\alpha\alpha')} g_d^{(\eta\eta')}(\mathbf{K})] d_{\eta\mathbf{K}\sigma}^{(\alpha)\dagger} d_{\eta'\mathbf{K}\sigma}^{(\alpha')} \\ & + \sum_{\mathbf{K}} [\varepsilon_f^{(m)} \delta_{mm'} + V_f^{(mm')} g_f(\mathbf{K})] f_{\eta\mathbf{K}\sigma}^{(m)\dagger} f_{\eta\mathbf{K}\sigma}^{(m')} \\ & + \sum_{\mathbf{K}} [V_{df}^{(\alpha m)} g_{df}^{(\eta\eta')}(\mathbf{K}) d_{\eta\mathbf{K}\sigma}^{(\alpha)\dagger} f_{\eta'\mathbf{K}\sigma}^{(m)} + \text{H.c.}] \\ & + \sum_{\mathbf{K}} [\sigma \Delta_{AF}^{(\alpha)} d_{\eta\mathbf{K}\sigma}^{(\alpha)\dagger} d_{\eta\mathbf{K}+\mathbf{Q}\sigma}^{(\alpha)} + \text{H.c.}] \\ & + U_f \sum_{\vec{r}_f} n_{f,\uparrow}^{(m)}(\vec{r}_f, \eta z_f) n_{f,\downarrow}^{(m)}(\vec{r}_f, \eta z_f). \end{aligned} \quad (4)$$

In the absence of d-electron ordering, Eq. (4) is the ALM with weak f-electron dispersion and momentum-dependent hybridization. (The effect of momentum-dependent hybridization on the Kondo effect has recently been studied in other contexts.[23,24]) For sufficiently large U_f, and with the f levels being well below Fermi energy, we are in the Kondo limit.

To concretely demonstrate how the d-electron AF order influences the Kondo effect, we consider the resulting Kondo lattice model with a single f-electron channel and two d-electron bands. In the slave-boson representation, this becomes

$$\begin{aligned} H_{KLM} = & \sum_{\mathbf{k}} \epsilon_d^{(\alpha\alpha')}(\mathbf{k}) d_{\mathbf{k}\sigma}^{(\alpha)\dagger} d_{\mathbf{k}\sigma}^{(\alpha')} + \lambda \left(\frac{1}{N_L} \sum_{\mathbf{k}} f_{\mathbf{k}\sigma}^\dagger f_{\mathbf{k}\sigma} - 1 \right) \\ & + \sum_{\mathbf{k}} [\sigma \Delta_{AF} d_{\mathbf{k}\sigma}^{(\alpha)\dagger} d_{\mathbf{k}+\mathbf{Q},\sigma}^{(\alpha)} + \text{H.c.}] \\ & - \frac{1}{2} J_K \sum_{\mathbf{k}} V_{df}(\mathbf{k}) b_\alpha [f_{\mathbf{k}\sigma}^\dagger d_{\mathbf{k}\sigma}^{(\alpha)} + \text{H.c.}]. \end{aligned} \quad (5)$$

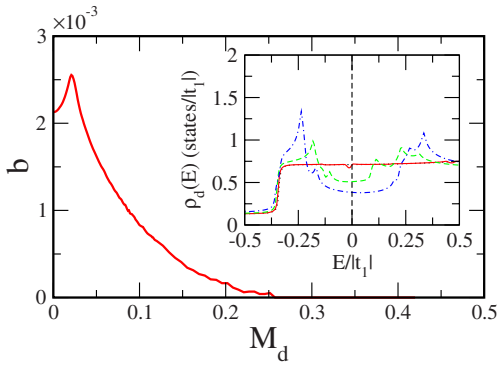

FIG. 2. (Color online) Mean-field Kondo parameter b as a function of the $\mathbf{Q}=(\pi,0)$ (in the notation of the one-Fe Brillouin zone) staggered magnetization M_d. The Kondo temperature $T_K \propto b^2$. M_d is measured in μ_B/Fe. The inset shows the d-electron density of states for $M_d=0$ (dotted black), 0.021 (solid red), 0.165 (dashed green), and 0.296 (dash-dotted blue).

Here, the Lagrange multiplier λ enforces the single occupancy of f electrons. The mean-field parameter $b_\alpha = \langle f^\dagger_{\mathbf{k}\sigma} d^{(\alpha)}_{\mathbf{k}\sigma}\rangle/2$ describes the Kondo screening and sets the Kondo scale, $T_K \propto b^2$. The anisotropic hybridization form factor $V_{df}(\mathbf{k})=4\cos k_x/2 \cos k_y/2$. The energy dispersion for d electrons is taken to be[25]

$$\epsilon^{(1)}(\mathbf{k}) = -2t_1 \cos k_x - 2t_2 \cos k_y - 4t_3 \cos k_x \cos k_y,$$

$$\epsilon^{(2)}(\mathbf{k}) = -2t_2 \cos k_x - 2t_1 \cos k_y - 4t_3 \cos k_x \cos k_y,$$

$$\epsilon^{(12)}(\mathbf{k}) = \epsilon^{(21)}(\mathbf{k}) = -4t_4 \sin k_x \sin k_y,$$

with $t_1=-1$, $t_2=1.3$, and $t_3=t_4=-0.85$. In our numerical study, we choose $J_K=0.04$, temperature $T=10^{-10}|t_1|$, and the lattice size $N_L=3200\times 3200$. When we vary the AF order parameter, the chemical potential is adjusted such that the d electrons are fixed at the half-filling $n_d=2.0$.

Figure 2 shows that the d-electron AF order rapidly suppresses the Kondo scale. This suppression is closely related to the depression of the d-electron density of states (DOS) in the collinear AF state of undoped iron arsenides (see the inset of Fig. 2). The feature of low-energy DOS is sensitive to the degree of nesting, and the DOS minimum is not necessarily located precisely at the Fermi energy (see, e.g., the case of $M_d=0.021$ in Fig. 2); the latter explains the effective Kondo scale first rising and then dropping with the AF order. Furthermore, the incomplete nesting of the Fermi surface keeps the depressed DOS finite (unlike, say, in the superconducting state) at the Fermi energy such that the $T=0$ ground state has the f moment always Kondo screened on the lattice.

We should stress that, for the purpose of a semiquantitative assessment of the proposed mechanism, we have considered the upper limit for the Kondo scale in the AF state: we have coupled the f moments to only the quasiparticles of the d electron AF state and have also neglected the f-moment ordering; moreover, a genuine f-electron quantum phase transition will be induced by breaking the Kondo screening upon the inclusion of the standard RKKY-Kondo competition.[26–28] We can therefore infer that the mechanism

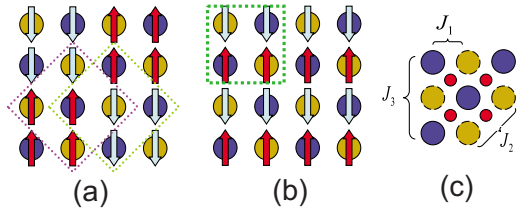

FIG. 3. (Color online) The would-be ordering patterns of the f electrons due to the superexchange interactions via (a) the R-X-R process alone or (b) the R-O-R process alone. (c) illustrates the combined exchanges, viewed as J_1-J_2-J_3 interactions of an *effective* square lattice within an RO layer, which are expected to turn the orders of (a) and (b) into a helical one. The big blue and brown circles label the rare-earth sites in the same way as in Fig. 1.

proposed here provides a viable basis to understand the distinct f-electron heavy-fermion behaviors in CeOFeP ($M_d \approx 0$) and CeOFeAs [$M_d \approx 0.8$ (Ref. 10)]. Our results also set the stage for understanding the evolution of the heavy-fermion behavior in the $CeOFeAs_{1-x}P_x$ series. In general, there will be two magnetic quantum critical points, x_{c_1} and x_{c_2}, associated with the d and f electrons, respectively. The RKKY interaction would then dominate in the intermediate region of x, leading likely to a ferromagnetic order before the heavy-fermion state is approached.

Magnetic frustration of the f electrons. We now turn to the exchange interactions among the f moments. Consider first the superexchange interaction, which can be derived by integrating out the virtual valence fluctuations of the f electrons. From Eq. (4), we end up with $\tilde{H}_f = \Sigma_{\vec{r}} J_f^{(m,m')} \vec{S}_F^{(m)}(\vec{r}_f, \eta z_f) \cdot \vec{S}_F^{(m')}(\vec{r}_f, \eta z_f)$, where $\vec{S}_F^{(m)}(\vec{r}, \eta z_f) = \Sigma_\square \vec{S}_f^{(m)}(\vec{r}_f, \eta z_f)$ are summations of f-electron spins in the corresponding plaquettes associated with $\vec{r}$, and $J_f^{(m,m')} \approx 2[V_f^{(mm')}]^2 (\frac{1}{U_f + \varepsilon_f^{(m)}} - \frac{1}{\varepsilon_f^{(m')}})$. This is the superexchange interaction associated with the R-X-R path, which does not mix the odd and even sublattices of the f sites in a single RO layer [see Fig. 3(a)]. There will also be a superexchange interaction from the R-O-R path due to the hybridization between the $4f$ orbitals of X atoms and the $2p$ orbitals of O atoms; this superexchange mixes the odd and even sublattices [see Fig. 3(b)]. In the notations of an effective square lattice of the f sites [cf. Fig. 3(c)] the R-O-R path gives rise to the nearest-neighbor (nn) interaction $J_1^{(O)}$ and the next-nearest neighbor (nnn) $J_2^{(O)}$, while the R-X-R path yields the nnn $J_2^{(X)}$ and the third-nearest neighbor (nnnn) $J_3^{(X)}$. (Note that $J_2^{(X)}$ and $J_3^{(X)}$ correspond to the nn and nnn interactions in the odd/even sublattices separately.) The resulting f-electron spin Hamiltonian becomes a J_1-J_2-J_3 Heisenberg model [Fig. 3(c)],

$$\mathcal{H}_f = \left\{ \sum_{\text{nn}} J_1 + \sum_{\text{nnn}} J_2 + \sum_{\text{nnnn}} J_3 \right\} \vec{S}_i \cdot \vec{S}_j, \tag{6}$$

where $J_1=J_1^{(O)}$, $J_2=J_2^{(O)}+J_2^{(X)}$, and $J_3=J_3^{(X)}$.

In this way, the f moments of CeOFeAs provide a realization of a geometrically frustrated quantum magnetic system in two dimensions. Quantum frustrated magnets have been the subject of theoretical studies for a long time and

continue to attract extensive interest.[29] However, suitable materials with spin-1/2 are rare. In this context, it will be very important to clarify the magnetic behavior of the f moments in CeOFeAs and related arsenides.

The $\vec{S}_F \cdot \vec{S}_F$ form given earlier corresponds to $J_3^{(X)}/J_2^{(X)}$ being equal to 1/2, and further bond-angle considerations imply that $J_3^{(X)}/J_2^{(X)}$ will be larger than 1/2 but still not far away from it. Similar considerations would suggest that $J_2^{(O)}/J_1^{(O)} \approx 1/2$. We will therefore expect $J_2 > J_1/2$ and a sizable J_3/J_1. In this range, the Néel and collinear orderings are excluded. Instead, an incommensurate helical phase with the ordering vector (q,π) or (q,q) is the most likely ground state, where $\cos q = \frac{2J_2 - J_1}{4J_3}$.[30] Neutron scattering and muon-spin-relaxation experiments in polycrystal CeOFeAs appear to have seen a helical f-electron ordering.[10,13] In the d-electron paramagnetic regime, there will also be an RKKY interaction. The latter is expected to be ferromagnetic given the relatively small size of the Fermi surfaces, and this is consistent with the enhanced ferromagnetic fluctuations of the heavy-fermion state observed in CeOFeP.[9] Still, the frustrating J_1-J_2-J_3 superexchange interactions will continue to operate, helping to suppress the tendency for AF ordering.

Discussion and summary. A number of other consequences of the p-f hybridization are relevant to the iron-pnictides phase diagram. First, in the heavy-fermion phase, the momentum dependence of the induced d-f hybridization will generally smear the hybridization gap (which has nodal lines along $\mathbf{K}_x = \pm \pi/a$ and $\mathbf{K}_y = \pm \pi/a$), and this could be visible in the optical-conductivity spectrum. Second, the induced d-f hybridization depends on the Fe-X and X-R distances. Increasing pressure along the c axis will decrease the distances and increase the hybridizations, and eventually enhance T_K.[11] Finally, in light of the fact that the f-electron ordering is further suppressed by the competing J_1-J_2-J_3 interactions, the transition or crossover from the superconducting to the heavy-fermion phases may take place at sufficiently high pressures in the carrier-doped superconducting materials.

In summary, we have considered a mechanism for weakening the Kondo screening effect through the antiferromagnetic order of the conduction electrons and implemented it in an extended Anderson lattice Hamiltonian. For the iron pnictides, our mechanism is semiquantitatively viable to explain the observed existence/absence of heavy-fermion behavior in CeOFeP and CeOFeAs, respectively. More broadly, our mechanism goes beyond the standard picture of heavy-fermion physics, viz., the RKKY and Kondo competition, and can therefore shed light on the phase diagram of heavy-fermion systems in general. Finally, we have proposed that the f electrons in the parent iron arsenides represent a rare model system for quantum frustrated magnetism in two dimensions.

We thank E. Abrahams, M. Aronson, G. H. Cao, X. H. Chen, X. Dai, C. Geibel, N. L. Wang, T. Xiang, Z. A. Xu, and H. Q. Yuan for useful discussions, and the U.S. DOE CINT at LANL for computational support. This work was supported by the NSF of China, the 973 Program, and the PCSIRT (Project No. IRT-0754) of Education Ministry of China (J.D.), by the NSF (Grant No. DMR-0706625) and the Robert A. Welch Foundation (Q.S.), and by the U.S. DOE at LANL under Contract No. DE-AC52-06NA25396 (J.-X.Z.).

[1] Y. Kamihara *et al.*, J. Am. Chem. Soc. **130**, 3296 (2008).
[2] G. F. Chen *et al.*, Phys. Rev. Lett. **100**, 247002 (2008).
[3] Z.-A. Ren *et al.*, EPL **82**, 57002 (2008).
[4] X. H. Chen *et al.*, Nature (London) **453**, 761 (2008).
[5] C. Wang *et al.*, EPL **83**, 67006 (2008).
[6] C. de la Cruz *et al.*, Nature (London) **453**, 899 (2008).
[7] Y. Kamihara *et al.*, J. Am. Chem. Soc. **128**, 10012 (2006); T. M. McQueen *et al.*, Phys. Rev. B **78**, 024521 (2008); J. J. Hamlin *et al.*, J. Phys.: Condens. Matter **20**, 365220 (2008).
[8] Y. Kamihara *et al.*, Phys. Rev. B **77**, 214515 (2008).
[9] E. M. Bruning *et al.*, Phys. Rev. Lett. **101**, 117206 (2008).
[10] J. Zhao *et al.*, Nature Mater. **7**, 953 (2008).
[11] L. Pourovskii *et al.*, EPL **84**, 37006 (2008).
[12] X. Dai (private communication).
[13] H. Maeter *et al.*, arXiv:0904.1563 (unpublished).
[14] S. Chi *et al.*, Phys. Rev. Lett. **101**, 217002 (2008).
[15] J. Dai *et al.*, Proc. Natl. Acad. Sci. U.S.A. **106**, 4118 (2009).
[16] P. Gegenwart *et al.*, Nat. Phys. **4**, 186 (2008).
[17] S. Doniach, Physica B & C **91**, 231 (1977); C. M. Varma, Rev. Mod. Phys. **48**, 219 (1976).
[18] R. Pottgen and D. Johrendt, Z. Naturforsch., B: Chem. Sci. **63**, 1135 (2008).
[19] C. Krellner *et al.*, Phys. Rev. Lett. **100**, 066401 (2008).
[20] Q. Si and E. Abrahams, Phys. Rev. Lett. **101**, 076401 (2008).
[21] T. Yildirim, Phys. Rev. Lett. **101**, 057010 (2008).
[22] F. Ma *et al.*, Phys. Rev. B **78**, 224517 (2008).
[23] P. Ghaemi *et al.*, Phys. Rev. B **77**, 245108 (2008).
[24] H. Weber and M. Vojta, Phys. Rev. B **77**, 125118 (2008).
[25] S. Raghu *et al.*, Phys. Rev. B **77**, 220503(R) (2008).
[26] Q. Si *et al.*, Nature (London) **413**, 804 (2001).
[27] T. Senthil *et al.*, Phys. Rev. B **69**, 035111 (2004).
[28] I. Paul, C. Pepin, and M. R. Norman, Phys. Rev. Lett. **98**, 026402 (2007).
[29] *Frustrated Spin Systems*, edited by H. T. Diep (World Scientific, Singapore, 2005).
[30] A. Moreo *et al.*, Phys. Rev. B **42**, 6283 (1990); M. P. Gelfand *et al.*, *ibid.* **40**, 10801 (1989).